ACS APPLIED MATERIALS & INTERFACES

Research Article

www.acsami.org

Fluorescent Nanohybrid of Gold Nanoclusters and Quantum Dots for Visual Determination of Lead Ions

Houjuan Zhu,[†,‡] Tao Yu,[§] Hongda Xu,[†,‡] Kui Zhang,[†] Hui Jiang,[§] Zhongping Zhang,[†] Zhenyang Wang,*[,†] and Suhua Wang*[,†,‡]

[†]Institute of Intelligent Machines, Chinese Academy of Sciences, Hefei, Anhui 230031, China

[‡]Department of Chemistry, University of Science & Technology of China, Hefei, Anhui 230026, China

[§]State Key Laboratory of NBC Protection for China, Research Institute of NBC Defense, Beijing, 102205, China

Supporting Information

ABSTRACT: Highly green emissive gold nanoclusters (Au NCs) are synthesized using glutathione as a stabilizing agent and mercaptopropionic acid as a ligand, and the intensity of fluorescence is specifically sensitive to lead ions. We then fabricated a ratiometric fluorescence nanohybrid by covalently linking the green Au NCs to the surface of silica nanoparticles embedded with red quantum dots (QDs) for on-site visual determination of lead ions. The green fluorescence can be selectively quenched by lead ions, whereas the red fluorescence is inert to lead ions as internal reference. The different response of the two emissions results in a continuous fluorescence color change from green to yellow that can be clearly observed by the naked eyes. The nanohybrid sensor exhibits high sensitivity to lead ions with a detection limit of 3.5 nM and has been demonstrated for determination of lead ions in real water samples including tap water, mineral water, groundwater, and seawater. For practical application, we dope the Au NCs in poly(vinyl alcohol) (PVA) film and fabricate fluorescence test strips to directly detect lead ions in water. The PVA-film method has a visual detection limit of 0.1 μM, showing its promising application for on-site identification of lead ions without the need for elaborate equipment.

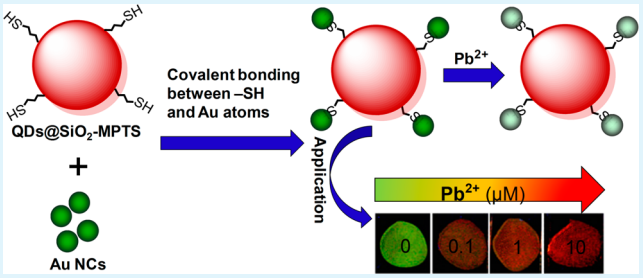

KEYWORDS: *visual detection, nanohybrid fluorescence sensor, lead ions, poly(vinyl alcohol) film, gold nanoclusters*

INTRODUCTION

Fluorescence materials have recently attracted much attention due to their advantages of sensitivity, simplicity, and low background signal for revealing trace amounts of analytes.[1−4] It is also considered to be a conceivable way to indicate the presence of an analyte that makes the changes of fluorescence color able to be observed by the naked eye.[5−9] Although fluorescent probes based on organic dyes have been extensively developed,[10−13] these organic dyes often require complicated synthesis and have narrow excitation and broad emission spectra. Recently, fluorescent nanomaterials have been employed for the design of new analytical methods because of their significantly improved optical properties and the ability for easy chemical functionalized modification.[14−17] Among the fluorescent nanomaterials reported to date, noble metal nanoclusters such as gold and silver clusters have attracted a great deal of attention owing to their ultrasmall sizes, low toxicity, and tunable fluorescent properties.[18−20] Recently, many different red fluorescence gold nanoclusters have been synthesized by stabilizing with protein, BSA, and lysozyme using the corresponding metal salt as precursors, while few green emissive gold nanoclusters have been reported except for a gold nanodot functionalized using mercaptoundecanoic acid (MUA).[21] However, the analytical performance of these fluorescence methods based on a single lumophore is generally dependent on probe concentration, excitation intensity, instrumental efficiency, and environmental conditions. Fortunately, the ratiometric fluorescence method employing two independent emissive bands as the signal possesses the advantages of self-calibration, built-in correction for environmental effects,[22−34] and visible color changes[35−37] potential for visual identification of target analytes. Therefore, it is practical to develop a novel dual-color fluorescence sensor based on ratiometric signal output for rapid visual identification of lead ions.

Lead compounds have been widely used in paint pigments, solders, storage batteries, water pipes, radiation shields, and ammunition and gasoline additives, leading to wide lead contamination and serious threat to environment and human health.[38,39] Lead is a kind of heavy metal element that is difficult to be chemically and biologically detoxified and hence easily accumulated in human nervous and cardiovascular systems when exposed to contaminated water sources and air.[40−43] In addition, lead ions can easily bond to the −SH

Received: September 19, 2014
Accepted: October 30, 2014
Published: October 30, 2014

   dx.doi.org/10.1021/am5064603 | ACS Appl. Mater. Interfaces 2014, 6, 21461−21467

Scheme 1. Schematic Illustration of the Ratiometric Probe Structure and the Visual Detection Principle for Lead Ions

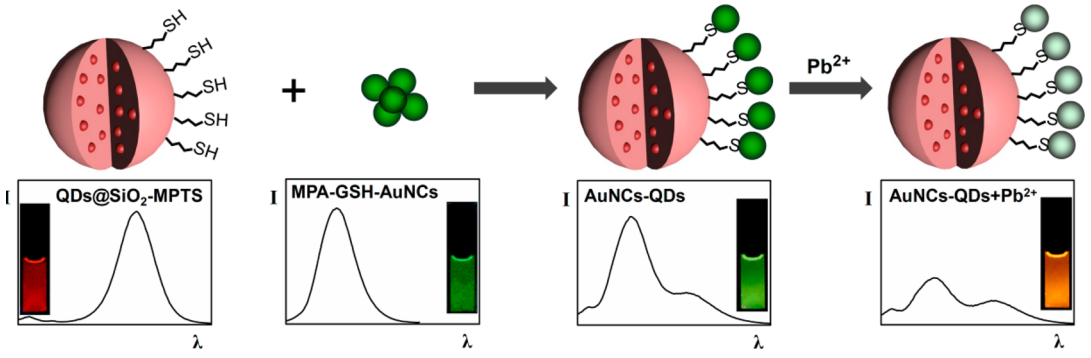

groups of enzymes or proteins and thus inhibit their activities once up-taken by the human body.[44−46] Therefore, the U.S. Environmental Protection Agency (EPA) has set the maximum allowable levels of lead in drinking water as 72 nM (15.0 ppb),[47] and the Centers for Disease Control and Prevention (CDC) also set the threshold for elevated blood lead at 480 nM (100 ppb).[48] Currently, several analytical methods have been employed for lead determination, such as atomic absorption spectrometry (AAS),[49,50] inductive coupled plasma atomic emission spectrometry (ICP-AES), anodic stripping voltammetry,[51] inductive coupled plasma mass spectrometry (ICP-MS).[52,53] These techniques often require expensive, sophisticated instrumentation and long sample preparation time, which hampers their practical application for in-field measurement.[54] Thus, it is necessary to develop a reliable, low-cost, rapid, on-site, and visual analytical technique for sensitive and selective determination of lead ions.

A few visual detection methods based on gold nanoparticles have recently been reported for lead ions detection with detection limit (LOD) at nanomolar level (Table S1, Supporting Information). These colorimetric methods generally use the dependence of localized surface plasmon resonance absorption of gold nanoparticles on their interparticle distances, which are very sensitive and vulnerable to surrounding condition variation, hence relatively low selectivity. Therefore, in this work, we combine gold nanoclusters (Au NCs) and quantum dots (QDs) embedded in silica nanoparticles to form a new ratiometric probe for visual identification of Pb^{2+} by fluorescence color changes. The dual-emission fluorescence nanohybrid probe has two emission peaks under a single-wavelength excitation, as illustrated in Scheme 1. The Au NCs emitting green fluorescence are covalently attached to the silica nanoparticle surface through the interaction between the gold atoms and the mercapto groups. The red-colored fluorescence of QDs is insensitive to Pb^{2+}, and the green-colored fluorescence of the Au NCs modified with glutathione (GSH) and mercaptopropionic acid (MPA) can be selectively quenched by Pb^{2+}. As the amounts of Pb^{2+} increase, the dual-emission intensity ratios gradually vary and lead to continuous changes of fluorescence color from green to yellow, which can be clearly observed by the naked eye. On the basis of the ratio and color change signatures, the ratiometric probe can be practically applied for both qualitative recognition and quantitative analysis. This method shows low interference and high selectivity with a detection limit of as low as 3.5 nM, which is much lower than the allowable level of lead (~72 nM) in drinking water (EPA).[45] Furthermore, we further apply the ratiometric probe for visual identification of Pb^{2+} in real water samples including tap water, mineral water, groundwater from Inner Mongolia, and seawater. In addition, a simple test device using poly(vinyl alcohol) (PVA) film doped with the ratiometric probe also has been successfully facilitated for on-site visual determination, and a detection limit of 0.1 μM has been estimated through the fluorescence color changes.

EXPERIMENTAL SECTION

Gold Nanoclusters Preparation. Green fluorescent Au NCs were synthesized according to the reported methods with minor modification.[21,55] Typically, 125 μL of 1 M NaOH solution and 3 μL of 80% tetrakis(hydroxymethyl)phosphonium chloride (THPC) solution were first introduced into 10 mL of ultrapure water. Then 125 μL of 0.1 M $HAuCl_4 \cdot 3H_2O$ solution was rapidly added into the mixture after stirring for 5 min. The color of the mixture turned from light yellow to brown in 1 min, indicating formation of small gold nanoparticles (Au NPs). At this point, 50 μL of 0.1 M GSH solution was added to obtain Au NPs protected by GSH. After stirring for another 15 min at room temperature, the stock Au NPs solution was kept at 4 °C for future use.

After aging for 1 day, 10 mL of the stock Au NPs solution was mixed with 1.8 mL of phosphate-buffered saline (PBS, 0.1 M) of pH 9.0 and 100 μL of MPA liquid. The mixture solution turned light yellow from brown within 24 h, indicating formation of fluorescent Au NCs. The Au NCs were purified by centrifugation and redispersed in water for future use. Absorption and emission spectra are shown in Figure S1, Supporting Information, and the fluorescence quantum yield was estimated to be 6.8% using fluorescein as standard (Figure S2, Supporting Information).[56]

Fabrication of Ratiometric Fluorescence Sensor. The red emissive QDs functionalized with mercapto groups were first bonded to the surface of Au NCs by a coordination reaction between −SH and Au atoms. In a typical procedure, 4 mL of green emissive Au NCs (λ_{em} = 520 nm) solution was mixed with 2 mL of 1 mg/mL of the mercaptopropyltrimethoxysilane (MPTS) modified silica nanoparticles under stirring in a 10 mL flask. The mixture was vigorously stirred for 2 h to form the nanohybrid. The resultant probes were collected by centrifugation and washed with ultrapure water three times to remove excess chemicals. The final product was dispersed in 6 mL of ultrapure water.

Measurement of Lead Ions. For aqueous Pb^{2+} detection, 1 mL of the as-synthesized ratiometric probes was injected into 1.0 mL of PBS (50 mM, pH = 6.0) in a spectrophotometer quartz cuvette. Then, 5, 10, 15, 20, 25, 30, 40, and 50 μL of lead ions (10^{-5} M) was added into the probe solution one by one, and the final concentrations of lead ions presented were 25, 50, 75, 100, 125, 150, 200, and 250 nM. The mixture was shaken thoroughly at room temperature prior to fluorescence measurement. Fluorescence spectra were collected 30 s after each addition because the fluorescence spectra became stable at 10 s after addition of lead ions. Spectra were measured by a fluorescence spectrophotometer (LS-55, PerkinElmer) excited at 390 nm. Fluorescence measurements were performed at room temperature under ambient conditions, and the average was obtained by three

independent measurements. Color changes were observed under a UV lamp (excitation wavelength at 365 nm).

Selectivity and Interference Experiments. Solutions of other metal ions were prepared in deionized (DI) water for the selectivity experiments except that mercuric ion was prepared in 0.1 M HNO_3 solution because it tends to hydrolyze in water. The fluorescent responses of the ratiometric probe to these metal ions were examined by a similar procedure used above for lead ions. The as-synthesized ratiometric probe solution and a series of selected metal ions (Cd^{2+}, Mg^{2+}, Ni^{2+}, Ca^{2+}, Co^{2+}, Ag^{+}, Cu^{2+}, Ba^{2+}, Hg^{2+}, Pb^{2+}, and Fe^{3+}; 50, 100, 150 nM) were mixed in 2.0 mL of PBS (25 mM, pH = 6.0). The mixtures were then added into a spectrophotometer quartz cuvette, and spectra were then measured at 390 nm excitation. For interference study, 150 nM Cd^{2+}, Mg^{2+}, Ni^{2+}, Ca^{2+}, Co^{2+}, Ag^{+}, Cu^{2+}, Ba^{2+}, Hg^{2+}, and Fe^{3+} were mixed with the probe in 2.0 mL of PBS (25 mM, pH = 6.0) followed by measuring the fluorescence spectra. Then, 75 nM Pb^{2+} was introduced into the mixture and the spectral responses were collected. Fluorescence images of these solutions were taken under a UV lamp with maximum output at 365 nm.

Analysis of Water Samples. Water samples included seawater, groundwater from Inner Mongolia, tap water, and mineral water. Seawater and groundwater were first filtered twice to remove any solid suspensions using ordinary qualitative filter membranes with 0.22 μm millipores (Sinopharm Chemical Reagent Co., Ltd.). Tap water was obtained from local drinking water, which was directly used without any pretreatment. Water samples spiked with different concentrations of Pb^{2+} were added to the sensing system, and the resultant fluorescence spectra were measured.

Construction of Ratiometric PVA-Film Sensor. In order to fabricate the PVA-film sensor, 5 g of PVA was first suspended in 100 mL of water in a flask. The mixture was then warmed at 90 °C in an oven to completely dissolve PVA. A clear aqueous solution of PVA was obtained after excess insoluble PVA was removed. The content of PVA in the clear solution was estimated to be 4.5%. The PVA solution was kept at room temperature in the dark for further use.

The nanohybrid probe solution (1 mL) was first centrifuged, and the precipitate was again dissolved into 50 μL of DI water. The purified probe solution was then mixed with 1 mL of the clear PVA solution, and the mixture was vigorously shaken to become homogeneous at room temperature. Glass slides were first washed in 10 mL of DI water by sonification for 10 min and then washed three times with DI water before drying. A 100 μL amount of the above mixture of probe and PVA was gently dripped onto a glass slide, which was transferred into an oven and dried at 50 °C for about 1 h to form the ratiometric PVA-film sensor.

On-Site Visual Measurement for Pb^{2+} on the Ratiometric PVA-Film Sensor. Lead solutions with concentrations of 10, 1, and 0.1 μM (10 mL) were prepared in dishes 5.5 cm in diameter. The PVA-film ratiometric sensors were immersed in the solutions for some time. Fluorescent photos of these films were taken once every 1 min under a UV lamp. The photostability of the PVA films with ratiometric probe and Au NCs were carefully examined and compared by monitoring their fluorescence spectra for about 1 h (Figures S3 and S4, Supporting Information).

RESULTS AND DISCUSSION

Preparation of the Green Emissive Gold Nanoclusters. Red fluorescent Au NCs have recently received much attention,[57−60] whereas green fluorescent Au NCs have been rarely reported. In this work, we synthesized Au NCs with green fluorescence using a multistep procedure. First, non-fluorescent THPC/GSH-stabilized/protected Au NPs or the "fluorescence off-state" Au NCs were synthesized during the Au(III) ion reduction in the presence of GSH together with THPC. Then MPA ligand was added for the subsequent ligand exchange reaction to produce the highly green fluorescent Au NCs.[33,55] The sizes of Au NCs, red QDs, and silica nanoparticles were, respectively, measured to be 2.3 (±0.2), 3.1 (±0.2), and 222 (±3) nm using TEM and SEM (Figure S5, Supporting Information). The green Au NCs show an emission peak centered at 520 nm (Figure S6a, Supporting Information), and a highly green fluorescence can be clearly observed under a UV lamp (λ_{ex} = 365 nm). The QDs-embedded silica nanoparticles have a fluorescence maximum at 620 nm and show strong red fluorescence under a UV lamp (Figure S6c, Supporting Information). Both the fluorescence spectra and the image of the ratiometric probe (Figure S6b, Supporting Information) are significantly different from those of the individual green Au NCs (Figure S6a, Supporting Information) and the red QDs (Figure S6c, Supporting Information) under a UV lamp. These results indicate that the green emissive AuNCs are successfully conjugated onto the surface of the red QD-embedded silica nanoparticles and both are photoluminescent under a single excitation.

Scheme 1 illustrates the architecture of the dual-emission fluorescence nanohybrid probe and the working principle for visually detecting lead ions. Red QDs are fully wrapped by the silica shell to improve their optical and chemical stabilities, which prevents direct contact of QDs with external Pb^{2+} and provides a reliable reference signal for the ratiometric probe. The surface of the silica nanoparticles is further functionalized with MPTS, and the end mercapto groups react with the surface of the green Au NCs.

The Au NCs act as recognition sites for Pb^{2+} through the affinity toward lead ions of two carboxyl groups and one amino group in glutathione on the surface of Au NCs,[31] resulting in the green fluorescence quenching, whereas the red fluorescence of the QD embedded in silica nanoparticles is inert to Pb^{2+}. Thus, the ratiometric fluorescence probe shows a clear color variation upon green fluorescence quenching by Pb^{2+}, while the red fluorescence intensity remains constant. A small variation of the ratio of the two intensities results in noticeable fluorescence color changes of the probe, hence facilitating visual detection of Pb^{2+} with the naked eye under a UV lamp. Furthermore, it has been demonstrated that the ratiometric probe was applied for building a ratiometric sensor to detect Pb^{2+} in real water samples.

Effect of pH on the Fluorescence of Gold Nanoclusters. The pH buffering systems are optimized by monitoring the fluorescence stability and reproducibility in PBS (25 mM). As shown in Figure 1, the fluorescence intensity ratios vary in the range of pH values from 4.0 to 8.5 due to the green fluorescence decrease of Au NCs with increasing pH values (Figures S7 and S8, Supporting Information), resulting in the variations of fluorescence color. Moreover, the fluorescence quenching efficiency of the ratiometric probe by lead ions is also studied at different pH values (Figures S9 and S10, Supporting Information). The ratiometric probe performs best in the pH range from 4 to 8.5 because the probe itself can be destroyed at very low pH condition and the metal ions can be hydrolyzed at high pH values. It can be clearly seen that the quenching efficiency increases below pH 6.0 and decreases as pH values increase. These results show that pH 6.0 is the most suitable condition for detection of lead ions. The photostability of the as-prepared ratiometric probe is systematically investigated by flashing UV light on the PBS solution of the ratiometric probe. After 10 consecutive illuminations with 2 min duration for each time, the relative fluorescence intensity has no apparent change, implying the high photostability in PBS solution (Figure S11, Supporting Information).

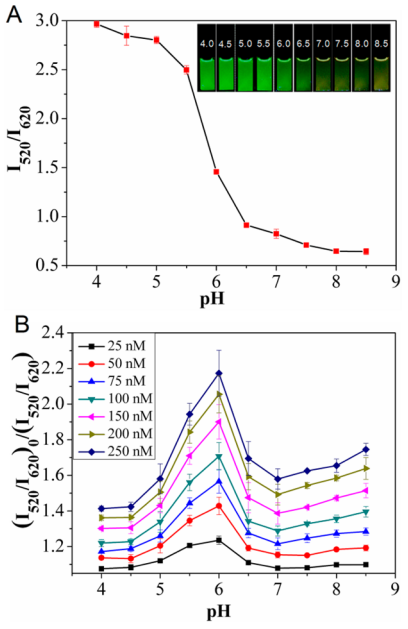

Figure 1. (A) Changes of the fluorescence intensity of the ratiometric probe upon different pH values in PBS (25 mM). (Inset) Fluorescence photos of the ratiometric probe were taken under a UV lamp with an excitation wavelength at 365 nm. (B) Plot of fluorescence quenching efficiency of the ratiometric probe as a function of pH value with addition of 25, 50, 75, 100, 150, 200, and 250 nM Pb^{2+}. $(I_{520}/I_{620})_0$ and (I_{520}/I_{620}) are the ratios of the fluorescence intensity of the ratiometric probe in the absence and presence of different concentrations of Pb^{2+}, respectively.

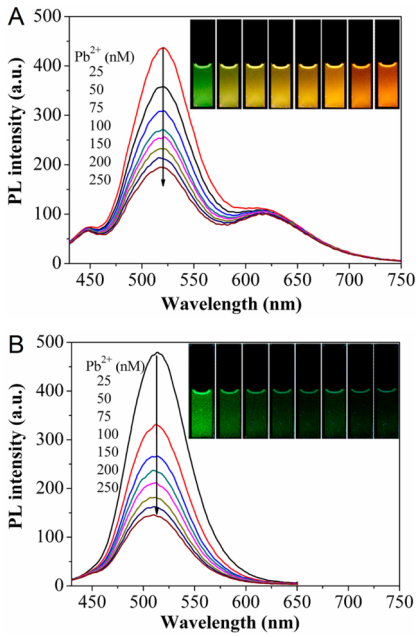

Figure 2. Fluorescence colors and the corresponding fluorescence spectra (λ_{ex} =390 nm) of (A) the ratiometric probe and (B) the pure green Au NCs upon exposure to different concentrations of Pb^{2+} in PBS (25 mM, pH = 6.0). Concentrations of Pb^{2+} from left to right are 0, 25, 50, 75, 100, 150, 200, and 250 nM. Fluorescence photos were taken under a UV lamp (excitation wavelength at 365 nm). The ratiometric fluorescence method shows clearer color changes than the single-wavelength fluorescence method.

Response of the Fluorescence of Gold Nanoclusters to Lead(II) Ions. To evaluate the sensitivity of the ratiometric probe, fluorescence responses are measured upon addition of different amounts of lead ions (Figure 2A). The fluorescence of the green Au NCs at 520 nm gradually decreases, whereas the fluorescence at 620 nm of the red QDs embedded in the silica nanoparticles still remains unchanged. With the increase of Pb^{2+} concentration, the changes in the intensity ratios of the two emission wavelengths lead to continuous variation of the fluorescence colors, as shown in the inset of Figure 2A. Clearly, a distinguishable color change from the original background could be observed upon even a slight decrease of the emission intensity at 520 nm, which is favorable for visual detection of Pb^{2+} by the naked eye. Figure 3 shows that the ratio of the fluorescence intensity continuously decreases with the increase of Pb^{2+} concentration, and it is closely related to the amount of Pb^{2+} from 2.5×10^{-8} to 2.5×10^{-7} M. A correlation can be established between $-\log[1.98 - (I_{520}/I_{620})_0/(I_{520}/I_{620})]$ and concentration throughout the entire concentration range of Pb^{2+}, and the coefficient is calculated to be 0.999. The detection limit is thus estimated to be as low as 3.5 nM (0.72 ppb) based on the definition of three times the deviation of the blank signal (3σ). The advantages of the ratiometric fluorescence probe for visual detection of Pb^{2+} can be clearly noted by comparison with the single-fluorescence quenching experiments (Figure S12, Supporting Information). Furthermore, the fluorescence color change of the pure Au NCs is hard to see by the naked eye (inset Figure 2). The comparison further demonstrates that the ratiometric fluorescence probe is more reliable for visual detection than a single-fluorescence quenching method.

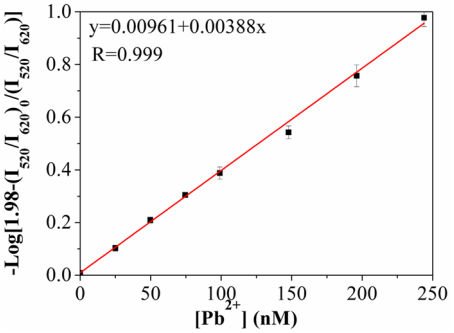

Figure 3. Plot of fluorescence quenching efficiency of the ratiometric probe as a function of the Pb^{2+} concentration in PBS (25 mM, pH = 6.0); detection limit of Pb^{2+} is calculated to be 3.5 nM on the basis of three times deviation.

Selectivity of Gold Nanoclusters for Detection of Lead Ions. To examine the selectivity of the ratiometric fluorescence probe, the effects of different kinds of metal ions on the fluorescence are investigated, including Cd^{2+}, Mg^{2+}, Ni^{2+}, Ca^{2+}, Co^{2+}, Ag^{+}, Cu^{2+}, Ba^{2+}, Hg^{2+}, and Fe^{3+}. Figure 4 shows the fluorescence intensity changes of the ratiometric fluorescence probe after adding different metal ions. It can be seen that the fluorescence intensity at 520 nm is gradually quenched to about 73.4%, 63.7%, and 59.1% by lead ions of 50, 100, and 150 nM, respectively. In contrast, addition of other metal ions do not lead to any obvious changes in the fluorescence intensity ratio and color, as shown in the inset of Figure 4. The results imply the high selectivity of the ratiometric fluorescence sensor for identification of Pb^{2+} over other metal ions. Moreover, we further examined the interference of other metal ions for Pb^{2+} detection by the following procedure. Metal ions (150 nM) mixed with 75 nM of Pb^{2+} were added into the probe solution,

dx.doi.org/10.1021/am5064603 | ACS Appl. Mater. Interfaces 2014, 6, 21461−21467

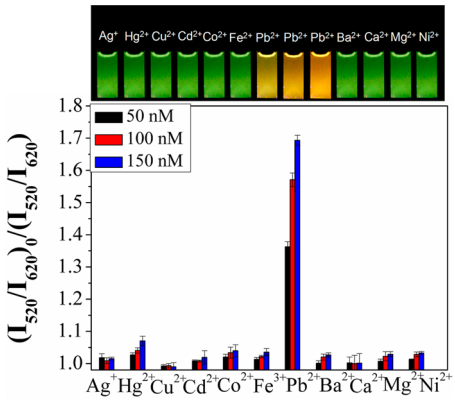

Figure 4. Selectivity of the ratiometric probe for Pb^{2+} over other metal ions in PBS (25 mM, pH = 6.0) including Ag^{+}, Hg^{2+}, Cu^{2+}, Cd^{2+}, Co^{2+}, Fe^{3+}, Ba^{2+}, Ca^{2+}, Mg^{2+}, and Ni^{2+} at concentrations of 50, 100, and 150 nM. Inset images show the corresponding fluorescence colors under a UV lamp.

followed by recording the fluorescence spectra. Clearly, there is no obvious interference observed for lead ions detection, even if the concentrations of the interfering ions are at least 2 times higher than that of Pb^{2+} (Figure 5). These results indicate that the coexistence of other metal ions indeed do not interfere with the measurement of Pb^{2+}.

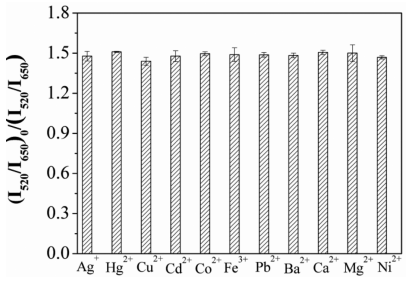

Figure 5. Interference of the ratiometric probe for 75 nM Pb^{2+} in PBS (25 mM, pH = 6.0) over other metal ions including 150 nM Ag^{+}, Hg^{2+}, Cu^{2+}, Cd^{2+}, Co^{2+}, Fe^{3+}, Ba^{2+}, Ca^{2+}, Mg^{2+}, and Ni^{2+}. No significant interference can be observed.

Detection of Lead(II) Ions in Real Water Samples. To further assess its applicability in real water samples, the ratiometric sensor was applied to detect Pb^{2+} in real water samples spiked with different amounts of Pb^{2+}, including seawater, groundwater from Inner Mongolia, tap water, and mineral water. Seawater and groundwater samples were first filtered to remove any solid suspensions, whereas tap water and mineral water samples were directly applied without any pretreatment. Studies were carried out with seven concentrations (25, 50, 75, 100, 150, 200, and 250 nM) spiked in each real sample. Each concentration was done in triplicate, and the averages were presented with standard deviation. Figure 6 shows the comparison of the fluorescence quenching efficiency by Pb^{2+} in different matrices of these water samples. Clearly, the fluorescence intensity ratios increase upon addition of Pb^{2+} for all of the real water samples. Furthermore, there are no significant differences in the data for detecting Pb^{2+} in seawater and groundwater when compared in deionized (DI) water, implying no serious interference to the probe. The recovery tests are performed in the four types of sample spiked with a fixed amount of lead ions, and the relative standard deviations

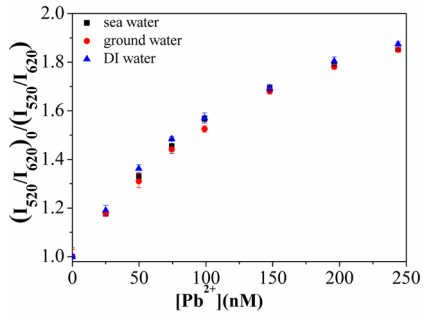

Figure 6. Fluorescence intensity ratios of the ratiometric probe as a function of the concentrations of Pb^{2+} (0, 25, 50, 75, 100, 150, 200, and 250 nM) spiked in different matrices of seawater, groundwater from Inner Mongolia, and DI water samples.

(RSD) are obtained by repeating the experiment 3 times. The measured recoveries of the tests and RSD are satisfactory, as shown in Table 1. It can be seen that the recoveries in real

Table 1. Recoveries of Lead Ions Spiked in Seawater, Groundwater, Tap Water, and Mineral Water by the Ratiometric Probe

	seawater			groundwater		
added Pb^{2+} (nM)	found Pb^{2+} (nM)	recovery (%)	RSD (%)	found Pb^{2+} (nM)	recovery (%)	RSD (%)
24.9	24.4	98.0	3.6	24.5	98.4	3.9
49.7	51.3	103.1	3.9	47.3	95.2	10
243.9	253.5	103.9	1.3	252.5	103.5	0.4
	mineral water			tap water		
added Pb^{2+} (nM)	found Pb^{2+} (nM)	recovery (%)	RSD (%)	found Pb^{2+} (nM)	recovery (%)	RSD (%)
24.9	28.0	112.4	5.0	27.2	109.2	9.8
49.7	49.9	100	6.3	48.2	97.0	4.0
243.9	254.5	104.5	2.5	233.5	95.8	6.5

water samples at concentrations of 24.9, 49.7, and 243.9 nM are statistically close to 100% (from 95% to 112%), indicating that the ratiometric fluorescence method performs well for lead ions determination in real water.

Fabrication of Fluorescent Sensor based on Gold Nanoclusters Doped PVA Film. We applied this probe for preparation of a practical sensor by the following procedure. The ratiometric fluorescence probe was first mixed with PVA in water to form a clear solution. The mixture solution was then dripped onto a glass slide, followed by drying in an oven at 50 °C. The fluorescence intensities of the PVA film of a ratiometric probe remain constant in 2 h, indicating its good photostability (Figure S4, Supporting Information). We then applied the sensors for visual detection of Pb^{2+} in water samples by immersing in target solutions with 10, 1, and 0.1 μM of lead ions for different times. Figure 7 clearly shows the dependence of fluorescence colors of the film probe on immersing time and concentration of lead ions. It can be seen that the fluorescence colors become stable at 11 min for the four water samples, suggesting that 11 min is enough for complete reaction. In addition, the fluorescence color quickly changes from yellow-green to red and becomes more pronounced for high concentrations of Pb^{2+} (10 μM). The visual detection limit is thus estimated as 0.1 μM, producing a least color variation that

dx.doi.org/10.1021/am5064603 | ACS Appl. Mater. Interfaces 2014, 6, 21461−21467

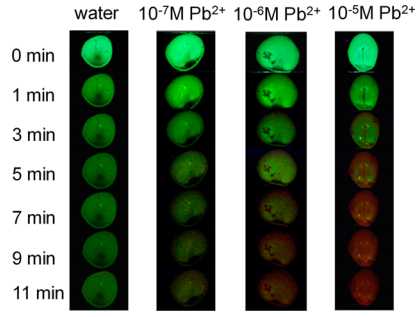

Figure 7. Fluorescence images of the PVA-film sensor for visual detection of trace Pb^{2+}. Prepared sensors were immersing into 0.1, 1, and 10 μM Pb^{2+} and DI water for comparison; images were taken every 1 min under a UV lamp under an excitation wavelength of 365 nm. Times indicate the duration of the film probe immersing in the target solutions.

can be easily noted by independent observers. These results demonstrate the utility of the film sensor for visual detection of trace residues of Pb^{2+}. The stability and practical utility of the film sensor were further examined by heating in an oven at 50 °C for 72 h, and it was found that the fluorescence color still remained the same (Figure S13, Supporting Information). The results show that the ratiometric PVA-film sensor has great potential for real water sample analysis with good reliability as well as on-site visual detection of lead residues in water.

CONCLUSION

We demonstrated a new concept and utility for visual detection of Pb^{2+} in aqueous solution. The concept utilizes a dual-color fluorescence nanohybrid probe, which is comprised of green-emissive Au NCs and red-emissive QDs embedded in silica nanoparticles, for determination of Pb^{2+} according to fluorescence color changes from green to yellow. This method exhibits significantly enhanced visual detection selectivity and reliability when compared with single Au NCs-based probes. Finally, the ratiometric fluorescence probe has been successfully applied to prepare test PVA film for efficient on-site visual determination of lead ions in complex real water samples.

ASSOCIATED CONTENT

Supporting Information

More detailed experiments including the preparation and surface modification of quantum dots embedding in silica nanoparticles. This material is available free of charge via the Internet at http://pubs.acs.org.

AUTHOR INFORMATION

Corresponding Authors

*E-mail: shwang@iim.ac.cn.
*E-mail: zywang@iim.ac.cn.

Notes

The authors declare no competing financial interest.

ACKNOWLEDGMENTS

This work was supported by the National Basic Research Program of China (2011CB933700) and the National Natural Science Foundation of China (Nos. 21205120, 21302187, 21475134).

REFERENCES

(1) Yu, Z. Q.; Schmaltz, R. M.; Bozeman, T. C.; Paul, R.; Rishel, M. J.; Tsosie, K. S.; Hecht, S. M. Selective Tumor Cell Targeting by the Disaccharide Moiety of Bleomycin. *J. Am. Chem. Soc.* **2013**, *135*, 2883−2886.
(2) Duong, T. Q.; Kim, J. S. Fluoro- and Chromogenic Chemodosimeters for Heavy Metal Ion Detection in Solution and Biospecimens. *Chem. Rev.* **2010**, *110*, 6280−6301.
(3) Du, J. J.; Hu, M. M.; Fan, J. L.; Peng, X. J. Fluorescent Chemodosimeters Using "Mild" Chemical Events for the Detection of Small Anions and Cations in Biological and Environmental Media. *Chem. Soc. Rev.* **2012**, *41*, 4511−4535.
(4) Sun, M. T.; Yu, H.; Zhu, H. J.; Ma, F.; Zhang, S.; Huang, D. J.; Wang, S. H. Oxidative Cleavage-Based Near-infrared Fluorescent Probe for Hypochlorous Acid Detection and Myeloperoxidase Activity Evaluation. *Anal. Chem.* **2014**, *86*, 671−677.
(5) Rakow, N. A.; Suslick, K.S. A Colorimetric Sensor Array for Odour Visualization. *Nature* **2000**, *406*, 710−713.
(6) Evans, R. C.; Douglas, P. Controlling the Color Space Response of Colorimetric Luminescent Oxygen Sensors. *Anal. Chem.* **2006**, *78*, 5645−5652.
(7) Evans, R. C.; Douglas, P. Design and Color Response of Colorimetric Multilumophore Oxygen Sensors. *ACS Appl. Mater. Interfaces* **2009**, *1*, 1023−1030.
(8) Witte, M. D.; Kallemeijn, W. W.; Aten, J.; Li, K. Y.; Strijland, A.; Donker-Koopman, W. E.; van den Nieuwendijk, A. M. C. H.; Bleijlevens, B.; Kramer, G.; Florea, B. I.; Hooibrink, B.; Hollak, C. E. M.; Ottenhoff, R.; Boot, R. G.; van der Marel, G. A.; Overkleeft, H. S.; Aerts, J. M. F. G. Ultrasensitive in Situ Visualization of Active Glucocerebrosidase Molecules. *Nat. Chem. Biol.* **2010**, *6*, 907−913.
(9) Yu, Z. Q.; Kabashima, T.; Tang, C. H.; Shibata, T.; Kitazato, K.; Kobayashi, N.; Lee, M. K.; Kai, M. Selective and Facile Assay of Human Immunodeficiency Virus Protease Activity by a Novel Fluorogenic Reaction. *Anal. Biochem.* **2010**, *397*, 197−201.
(10) Xu, H. R.; Li, K.; Liu, Q.; Wu, T. M.; Wang, M. Q.; Hou, J. T.; Huang, Z.; Xie, Y. M.; Yu, X. Q. Dianthracene-Cyclen Conjugate: the First Equal-Equivalent Responding Fluorescent Chemosensor for Pb^{2+} in Aqueous Solution. *Analyst* **2013**, *138*, 2329−2334.
(11) Liu, J.; Wu, K.; Li, S.; Song, T.; Han, Y. F.; Li, X. A Highly Sensitive and Selective Fluorescent Chemosensor for Pb^{2+} Ions in an Aqueous Solution. *Dalton Trans.* **2013**, *42*, 3854−3859.
(12) Chen, C. T.; Huang, W. P. A Highly Selective Fluorescent Chemosensor for Lead Ions. *J. Am. Chem. Soc.* **2002**, *124*, 6246−6247.
(13) Kwon, J. Y.; Jang, Y. J.; Lee, Y. J.; Kim, K. M.; Seo, M. S.; Nam, W.; Yoon, J. A Highly Selective Fluorescent Chemosensor for Pb^{2+}. *J. Am. Chem. Soc.* **2005**, *127*, 10107−10111.
(14) Cai, Z. X.; Shi, B. Q.; Zhao, L.; Ma, M. H. Ultrasensitive and Rapid Lead Sensing in Water Based on Environmental Friendly and High Luminescent L-Glutathione-Capped-ZnSe Quantum Dots. *Spectrochim. Acta, Part A* **2012**, *97*, 909−914.
(15) Li, M.; Zhou, X. J.; Guo, S. W.; Wu, N. Q. Detection of Lead (II) with a "Turn-on" Fluorescent Biosensor Based on Energy Transfer from CdSe/ZnS Quantum Dots to Graphene Oxide. *Biosens. Bioelectron.* **2013**, *43*, 69−74.
(16) Liu, B. H.; Han, G. M.; Zhang, Z. P.; Liu, R. Y.; Jiang, C. L.; Wang, S. H.; Han, M. Y. Shell Thickness-Dependent Raman Enhancement for Rapid Identification and Detection of Pesticide Residues at Fruit Peels. *Anal. Chem.* **2012**, *84*, 255−261.
(17) Tu, R. Y.; Liu, B. H.; Wang, Z. Y.; Gao, D. M.; Wang, F.; Fang, Q. L.; Zhang, Z. P. Amine-Capped ZnS-Mn^{2+} Nanocrystals for Fluorescence Detection of Trace TNT Explosive. *Anal. Chem.* **2008**, *80*, 3458−3465.
(18) Zheng, J.; Nicovich, P. R.; Dickson, R. M. Highly Fluorescent Noble-Metal Quantum Dots. *Annu. Rev. Phys. Chem.* **2007**, *58*, 409−431.
(19) Guo, W. W.; Yuan, J. P.; Wang, E. K. Oligonucleotide-Stabilized Ag Nanoclusters as Novel Fluorescence Probes for the Highly Selective and Sensitive Detection of the Hg^{2+} Ion. *Chem. Commun.* **2009**, *27*, 3395−3397.

(20) Huang, C. C.; Yang, Z.; Lee, K. H.; Chang, H. T. Synthesis of Highly Fluorescent Gold Nanoparticles for Sensing Mercury(II). *Angew. Chem.Int. Ed.* **2007**, *46*, 6824−6828.
(21) Yuan, Z. Q.; Peng, M. H.; He, Y.; Yeung, E. S. Functionalized Fluorescent Gold Nanodots: Synthesis and Application for Pb^{2+} Sensing. *Chem. Commun.* **2011**, *47*, 11981−11983.
(22) Snee, P. T.; Somers, R. C.; Nair, G.; Zimmer, J. P.; Bawendi, M. G.; Nocera, D. G. A Ratiometric CdSe/ZnS Nanocrystal pH Sensor. *J. Am. Chem. Soc.* **2006**, *128*, 13320−13321.
(23) Shynkar, V. V.; Klymchenko, A. S.; Kunzelmann, C.; Duportail, G.; Muller, C. D.; Demchenko, A. P.; Freyssinet, J. M.; Mely, Y. Fluorescent Biomembrane Probe for Ratiometric Detection of Apoptosis. *J. Am. Chem. Soc.* **2007**, *129*, 2187−2193.
(24) Wang, M.; Mei, Q. S.; Zhang, K.; Zhang, Z. P. Protein-Gold Nanoclusters for Identification of Amino Acids by Metal Ions Modulated Ratiometric Fluorescence. *Analyst* **2012**, *137*, 1618−1623.
(25) Kubo, Y.; Yamamoto, M.; Ikeda, M.; Takeuchi, M.; Shinkai, S.; Yamaguchi, S.; Tamao, K. A Colorimetric and Ratiometric Fluorescent Chemosensor with Three Emission Changes: Fluoride Ion Sensing by a Triarylborane-Porphyrin Conjugate. *Angew. Chem., Int. Ed.* **2003**, *42*, 2036−2040.
(26) Wu, P.; Zhao, T.; Wang, S. L.; Hou, X. D. Semicondutor Quantum Dots-Based Metal Ion Probes. *Nanoscale* **2014**, *6*, 43−64.
(27) Sen, S.; Sarkar, S.; Chattopadhyay, B.; Moirangthem, A.; Basu, A.; Dhara, K.; Chattopadhyay, P. A Ratiometric Fluorescent Chemosensor for Iron: Discrimination of Fe^{2+} and Fe^{3+} and Living Cell Application. *Analyst* **2012**, *137*, 3335−3342.
(28) Woodroofe, C. C.; Lippard, S. J. A Novel Two-Fluorophore Approach to Ratiometric Sensing of Zn^{2+}. *J. Am. Chem. Soc.* **2003**, *125*, 11458−11459.
(29) Han, Z. X.; Zhang, X. B.; Zhuo, L.; Gong, Y. J.; Wu, X. Y.; Zhen, J.; He, C. M.; Jian, L. X.; Jing, Z.; Shen, G. L.; Yu, R. Q. Efficient Fluorescence Resonance Energy Transfer-Based Ratiometric Fluorescent Cellular Imaging Probe for Zn^{2+} Using a rRhodamine Spirolactam as a Trigger. *Anal. Chem.* **2010**, *82*, 3108−3113.
(30) Gong, Y. J.; Zhang, X. B.; Zhang, C. C.; Luo, A. L.; Fu, T.; Tan, W. H.; Shen, G. L.; Yu, R. Q. Through Bond Energy Transfer: a Convenient and Universal Strategy toward Efficient Ratiometric Fluorescent Probe for Bioimaging Applications. *Anal. Chem.* **2012**, *84*, 10777−10784.
(31) Wu, C. F.; Bull, B.; Christensen, K.; McNeill, J. Ratiometric Single-Nanoparticle Oxygen Sensors for Biological Imaging. *Angew. Chem., Int. Ed.* **2009**, *48*, 2741−2745.
(32) Wang, Z.; Palacios, M. A.; Zyryanov, G.; Anzenhacher, P. Harnessing a Ratiometric Fluorescence Output from a Sensor Array. *Chem.—Eur. J.* **2008**, *14*, 8540−8546.
(33) Haidekker, M. A.; Brady, T. P.; Lichlyter, D.; Theodorakis, E. A. A Ratiometric Fluorescent Viscosity Sensor. *J. Am. Chem. Soc.* **2006**, *128*, 398−399.
(34) Doussineau, T.; Schulz, A.; Lapresta-Fernandez, A.; Moro, A.; Körsten, S.; Trupp, S.; Mohr, G. J. On the Design of Fluorescent Ratiometric Nanosensors. *Chem.—Eur. J.* **2010**, *16*, 10290−10299.
(35) Zhang, K.; Zhou, H. B.; Mei, Q. S.; Wang, S. H.; Guan, G. J.; Liu, R. Y.; Zhang, J.; Zhang, Z. P. Instant Visual Detection of Trinitrotoluene Particulates on Various Surfaces by Ratiometric Fluorescence of Dual-emission Quantum Dots Hybrid. *J. Am. Chem. Soc.* **2011**, *133*, 8424−8427.
(36) Yao, J. L.; Zhang, K.; Zhu, H. J.; Ma, F.; Sun, M. T.; Yu, H.; Sun, J.; Wang, S. H. Efficient Ratiometric Fluorescence Probe Based on Dual-Emission Quantum Dots Hybrid for on-Site Determination of Copper Ions. *Anal. Chem.* **2013**, *85*, 6461−6468.
(37) Zhu, H. J.; Zhang, W.; Zhang, K.; Wang, S. H. Dual-Emission of a Fluorescent Graphene Oxide-Quantum Dot Nanohybrid for Sensitive and Selective Visual Sensor Applications Based on Ratiometric Fluorescence. *Nanotechnology* **2012**, *23*, 315502.
(38) Yang, S. B.; Hu, J.; Chen, C. L.; Shao, D. D.; Wang, X. K. Mutual Effect of Pb(II) and Humic Acid Adsorption onto Multiwalled Carbon Nanotubes/Poly(acrylamide) Composites from Aqueous Solution. *Environ. Sci. Technol.* **2011**, *45*, 3621−3627.
(39) Zhao, G. X.; Li, J. X.; Ren, X. M.; Chen, C. L.; Wang, X. K. Few-layered Graphene Oxide Nanosheets as Superior Sorbents for Heavy Metal Ion Pollution Management. *Environ. Sci. Technol.* **2011**, *45*, 10454−10462.
(40) Zhang, K.; Yang, L.; Zhu, H. J.; Ma, F.; Zhang, Z. P.; Wang, S. H. Selective Visual Detection of Trace Trinitrotoluene Residues Based on Dual-Color Fluorescence of Graphene Oxide-Nanocrystals Hybrid Probe. *Analyst* **2014**, *139*, 2379−2385.
(41) Liew, J.; Goyer, R. A.; Waalkes, M. P. Toxic Effects of Metals. In *Casarett and Doull's Toxicology: The Basic Science of Poisons*; Klaassen, C. D., Ed.; *Casarett and Doull's Toxicology: The Basic Science of Poisons*; The Mc Graw-Hil Companies Inc.: New York, 2008; p 931.
(42) Fen, Y. W.; Mat Yunus, W. M.; Talib, Z. A. Analysis of Pb(II) Ion Sensing by CrosslinkedChitosan Thin Film Using Surface Plasmon Resonance Spectroscopy. *Optik* **2013**, *124*, 126−133.
(43) Schwartz, J. Societal Benefits of Reducing Lead Exposure. *Environ. Res.* **1994**, *66*, 105−124.
(44) Goyer, R. A. Lead Toxicity: from Overt to Subclinical to Subtle Health Effects. *Environ. Health Perspect.* **1990**, *86*, 177−181.
(45) Gonick, H. C.; Behari, J. R. Is Lead Exposure the Principal Cause of Essential Hypertension? *Med. Hypotheses* **2002**, *59*, 239−246.
(46) Dietert, R. R.; Lee, J. E.; Hussain, I.; Piepenbrink, M. Developmental Immunotoxicology of Lead. *Toxicol. Appl. Pharmacol.* **2004**, *198*, 86−94.
(47) EPA 816-F-09-0004, U.S. EPA, 2009.
(48) US Department of Health and Human Services, Centers for Disease Control and Prevention: Atlanta, GA.
(49) Parsons, P. J.; Slavin, W. A Rapid Zeeman Graphite Furnace Atomic Absorption Spectrometric Method for the Determination of Lead in Blood. *Spectrochim. Acta, Part B* **1993**, *48*, 925−939.
(50) Tahan, J. E.; Granadillo, V. A.; Romero, R. A. Electrothermal Atomic Absorption Spectrometric Determination of Al, Cu, Fe, Pb, V and Zn in Clinical Samples and in Certified Environmental Reference Materials. *Anal. Chim. Acta* **1994**, *295*, 187−197.
(51) Feldman, B. J.; Osterloh, J. D.; Hata, B. H.; D'Alessandro, A. Determination of Lead in Blood by Square Wave Anodic Stripping Voltammetry at a Carbon Disk Ultramicroelectrode. *Anal. Chem.* **1994**, *66*, 1983−1987.
(52) Liu, H. W.; Jiang, S. J.; Liu, S. H. Determination of Cadmium, Mercury and Lead in Seawater by Electrothermal Vaporization Isotope Dilution Inductively Coupled Plasma Mass Spectrometry. *Spectrochim. Acta, Part B* **1999**, *54*, 1367−1375.
(53) Bowins, R. J.; McNutt, R. H. J. Electrothermal Isotope Dilution Inductively Coupled Plasma Mass Spectrometry Method for the Determination of Sub-ng/mL Levels of Lead in Human Plasma. *J. Anal. At. Spectrom.* **1994**, *9*, 1233−1236.
(54) Jain, A. K.; Gupta, V. K.; Singh, L. P.; Raisoni, J. R. A Comparative Study of Pb^{2+} Selective Sensors Based on Derivatized Tetrapyrazole and Calix[4]arene Receptors. *Electrochim. Acta* **2006**, *51*, 2547−2553.
(55) Huang, C. C.; Liao, H. Y.; Shiang, Y. C.; Lin, Z. H.; Yang, Z. S.; Chang, H. T. Synthesis of Wavelength-Tunable Luminescent Gold and Gold/Silver Nanodots. *J. Mater. Chem.* **2009**, *19*, 755−759.
(56) Brouwer, A. M. Standards for Photoluminescence Quantum Yield Measurements in Solution. *Pure Appl. Chem.* **2011**, *83*, 2213−2228.
(57) Xie, J. P.; Zheng, Y. G.; Ying, J. Y. Highly Selective and Ultrasensitive Detection of Hg^{2+} Based on Fluorescence Quenching of Au Nanoclusters by Hg^{2+}-Au^{+} Interactions. *Chem. Commun.* **2010**, *46*, 961−963.
(58) Wei, H.; Wang, Z. D.; Yang, L. M.; Tian, S. L.; Hou, C. J.; Lu, Y. Lysozyme-sStabilized Gold Fluorescent Cluster: Synthesis and Application as Hg^{2+} Sensor. *Analyst* **2010**, *135*, 1406−1410.
(59) Durgadas, C. V.; Sharma, C. P.; Sreenivasan, K. Fluorescent Gold Clusters as Nanosensors for Copper Ions in Live Cells. *Analyst* **2011**, *136*, 933−940.
(60) Shang, L.; Brandholt, S.; Stockmar, F.; Trouillet, V.; Bruns, M.; Nienhaus, G. U. Effect of Protein Adsorption on the Fluorescence of Ultrasmall Gold Nanoclusters. *Small* **2012**, *8*, 661−665.